

**ORIGINAL
RESEARCH**

C. Ryberg
E. Rostrup
K. Sjöstrand
O.B. Paulson
F. Barkhof
P. Scheltens
E.C.W. van Straaten
F. Fazekas
R. Schmidt
T. Erkinjuntti
L.-O. Wahlund
A.M. Basile
L. Pantoni
D. Inzitari
G. Waldemar,
on behalf of the
LADIS study group

White Matter Changes Contribute to Corpus Callosum Atrophy in the Elderly: The LADIS Study

BACKGROUND AND PURPOSE: The corpus callosum (CC) is the most important structure involved in the transmission of interhemispheric information. The aim of this study was to investigate the potential correlation between regional age-related white matter changes (ARWMC) and atrophy of CC in elderly subjects.

MATERIALS AND METHODS: In 578 subjects with ARWMC from the Leukoaraiosis And Disability (LADIS) study, the cross-sectional area of the CC was automatically segmented on the normalized midsagittal MR imaging section and subdivided into 5 regions. The ARWMC volumes were measured quantitatively by using a semiautomated technique and segmented into 6 brain regions.

RESULTS: Significant correlation between the area of the rostrum and splenium regions of the CC and the ARWMC load in most brain regions was identified. This correlation persisted after correction for global atrophy.

CONCLUSION: Increasing loads of ARWMC volume were significantly correlated with atrophy of the CC and its subregions in nondisabled elderly subjects with leukoaraiosis. However, the pattern of correlation between CC subregions and ARWMC was not specifically related to the topographic location of ARWMC. The results suggest that ARWMC may lead to a gradual loss of CC tissue.

The corpus callosum (CC) is the most important commissural tract in the brain containing myelinated axons transversing the subcortical white matter. The CC serves to unite the 2 hemispheres anatomically and functionally, and CC atrophy may be associated with cognitive and motor deficits.¹⁻⁵ A gradual decline in the area and width of the CC has been reported after the fourth decade of life.⁶

There is a considerable interindividual variability in the area and shape of the CC in the healthy elderly. Both positive and negative results have been obtained regarding the correlation of CC cross-sectional areas to factors such as sex and handedness,⁷⁻¹⁵ number of lacunes and the presence of infarcts in the cerebral hemispheres,^{16,17} and/or brain size.¹⁸

The mechanism for CC atrophy is poorly understood, but

CC atrophy may reflect pathologic changes in subcortical white matter, as reported in patients with multiple sclerosis¹⁹ and vascular dementia.²⁰ In healthy elderly subjects, CC atrophy may result from axonal disruption due to white matter damage.

The association between age-related white matter changes (ARWMC) and CC atrophy was previously examined in 5 studies of the elderly with leukoaraiosis,²¹ infarcts and cardiovascular risk factors,¹⁶ Alzheimer disease (AD),²¹⁻²³ and healthy elderly controls.^{16,21-23} Each of these studies was based on relatively small sample sizes, and taken together, they have not provided a common conclusion concerning the potential influence of ARWMC on the size of the CC. For example, in 3 studies analyzing MR imaging from patients with AD, 1 study ($N = 15$) found significant correlation between ARWMC and CC atrophy, whereas 2 studies ($N = 21$ and $N = 29$) did not find any significant correlation.^{22,23} In healthy elderly controls, 3^{21,22} of 4 studies ($n \leq 29$)^{16,21-23} found a significant correlation between ARWMC and CC atrophy. The same association was found in a population with cardiovascular risk factors ($n = 14$) and infarcts ($n = 30$).¹⁶ However, in the population of elderly subjects with leukoaraiosis ($N = 62$), Yamauchi et al (2000)²⁴ did not find any significant correlation between ARWMC and CC atrophy.

The contradictory conclusions could be due to the use of different methods for segmentation and subdivision of the CC or to different rating techniques for assessment of ARWMC and CC. Small populations and the use of subjective rating scales may obscure potential correlations.

The aim of this study was to investigate the correlation between regional ARWMC and atrophy of CC subregions in a large population of nondisabled elderly subjects with leukoaraiosis.

Received February 26, 2008; accepted after revision April 14.

From the Memory Disorders Research Group (C.R., G.W.), Department of Neurology, Copenhagen University Hospital, Copenhagen, Denmark; Danish Research Center for Magnetic Resonance (C.R., E.R., O.B.P.), Copenhagen University Hospital, Hvidovre, Denmark; Informatics and Mathematical Modelling (K.S.), Technical University of Denmark, Copenhagen, Denmark; Neurobiology Research Unit (O.B.P.), Copenhagen University Hospital, Rigshospitalet, Copenhagen, Denmark; Departments of Radiology and Image Analysis Center (F.B.) and Neurology (P.S., E.C.W.v.S.), VU Medical Center, Amsterdam, the Netherlands; Department of Neurology (F.F., R.S.), Medical University, Graz, Austria; Memory Research Unit (T.E.), Department of Neurology, University of Helsinki, Helsinki, Finland; Department of Clinical Neuroscience (L.-O.W.), NEUROTEC, Karolinska Institute, Huddinge University Hospital, Stockholm, Sweden; and Department of Neurological and Psychiatric Sciences (A.M.B., L.P., D.I.), University of Florence, Florence, Italy.

This work was supported by the European Union (grant QLRT-2000-00446, Impact of age-related brain white matter changes on transition to disability in the elderly: Leukoaraiosis and Disability); the Danish Velux Foundation; and the Danish Alzheimer Research Foundation.

Please address correspondence to Gunhild Waldemar, MD, DMSc, Department of Neurology, Section 2082, The Copenhagen Memory Clinic & The Memory Disorders Research Group, Rigshospitalet, Copenhagen University Hospital, 9 Blegdamsvej, DK 2100, Copenhagen, Denmark; e-mail: gunhild.waldemar@rh.regionh.dk

DOI 10.3174/ajnr.A1169

Materials and Methods

Patient Selection

The study included 639 (mean age, 74.1 ± 5 years; female/male ratio, 351/288) subjects from a mixed elderly population with ARWMC who participated in the longitudinal European multicenter study Leukoaraiosis And Disability in the elderly (LADIS) described in detail elsewhere.²⁵ The study involved a total of 11 European centers, either specialized memory clinics or geriatric or neurologic departments with a similar specialization. Briefly, the objective of the LADIS study was to assess the role of ARWMC as an independent predictor of the transition to disability in the initially nondisabled elderly and to describe health-related consequences of ARWMC. The study was approved by the relevant ethics committees for all participating centers.

The LADIS subjects had different grades of ARWMC and no or only minor disability as assessed with the Instrumental Activities of Daily Living (IADL).²⁶ The enrolled subjects had been referred to neurologic, psychiatric, or geriatric departments in most cases (80%) due to various mild complaints, including mild cognitive symptoms, minor cerebrovascular events, or other neurologic complaints. About 10% of the participants were healthy elderly controls from other studies, and in a few cases, contact was made due to complaints of gait disturbance or mood alterations (minor depression). The ARWMC were initially identified on their cranial MR imaging or CT. The LADIS aimed to have a balanced enrollment regarding the severity of ARWMC based on the Fazekas score.²⁷

The criteria for inclusion were the following: 1) age between 64 and 85 years, 2) presence of ARWMC on MR imaging or CT, 3) no or only mild functional disability determined by the IADL scale (IADL score ≤ 1), 4) the presence of a regularly contactable informant, and 5) informed consent.

Exclusion criteria were the following: 1) subject likely to drop out because of the presence of severe illness (cardiac, hepatic, or renal failure; cancer; or other relevant systemic diseases), 2) severe unrelated neurologic diseases, 3) leukoencephalopathy of nonvascular origin (immunologic-demyelinating, metabolic, toxic, infectious, other), 4) severe psychiatric disorders, 5) inability to give an informed consent, and 6) inability or refusal to undergo cerebral MR imaging.

All subjects underwent a medical interview, clinical examination, and MR imaging. The present article was based on the baseline clinical and MR imaging data.

MR Imaging

The MR imaging protocol consisted of 3D sagittal or coronal T1-weighted magnetization-prepared rapid acquisition of gradient echo (MPRAGE) images (TE = 4–7 ms, TR = 10–25 ms, TI = 100–950 ms, flip angle = 10° – 30° , voxel size = $1 \times 1 \times 1.5$ mm³, FOV = 250 mm), axial T2-weighted fast spin-echo (FSE) images (TE = 100–120 ms, TR = 4000–6000 ms, FOV = 250 mm), and fluid-attenuated inversion recovery (FLAIR) images (TE = 100–140 ms, TR = 6000–10,000 ms, TI = 2000–2400 ms, FOV = 250 mm). For the FSE and FLAIR measurements, the in-plane resolution was 1×1 mm and the section thickness ranged from 5 to 7.5 mm (section gap, 0.5 mm). The scans were acquired on 0.5T (1 center) or 1.5T scanners (10 centers).

Of the 639 subjects included in the LADIS study, only 578 (female/male ratio, 313/265) had undergone MR imaging, which allowed segmentation of the CC and subsequent comparison of MR imaging with clinical data (Tables 1 and 2). A total of 61 subjects were excluded due to the following: The MPRAGE dataset was unavailable or incomplete in 43 subjects or of insufficient

Table 1: Clinical and MR imaging characteristics (N = 578)*

Characteristic	No.
Female	313 (54%)
Age (years)	74.1 (± 5)
MMSE score (0–30)	27.4 (± 2)
Handedness (No. of subjects)†	
Left	27 (4.7%)
Right	524 (90.8%)
Ambidextrous	26 (4.5%)
ARWMC ratings (No. of subjects)	
Mild (score 1)	260 (45%)
Moderate (score 2)	178 (31%)
Severe (score 3)	140 (24%)
ARWMC volume (mL)	
Mild (score 1)	7.3 (± 5.3)
Moderate (score 2)	21.5 (± 8.2)
Severe (score 3)	58.4 (± 27.2)
No. of lacunes (No. of subjects)	
0	308 (47%)
1–3	195 (34%)
≥ 4	75 (13%)
No. of infarcts (No. of subjects)	
0	523 (90%)
1	43 (7%)
≥ 2	12 (3%)

Note:—MMSE indicates Mini-Mental State Examination; ARWMC, age-related white matter changes.

* Values are mean (\pm SD) or numbers (percentages).

† Available for $n = 577$.

quality (6 subjects); or the FLAIR dataset was unavailable or incomplete (5 subjects) or of insufficient quality (3 subjects); and 4 subjects were excluded due to lack of relevant clinical data such as sex, age, and handedness.

Assessment of ARWMC Load, Lacunes, and Infarcts

Definition of Anatomic Regions of the Brain. Anatomic regions (frontal, parietal, temporal, occipital, basal ganglia, and infratentorial region) were manually defined by using definitions from anatomic atlases on a T1-weighted template (Fig 1). The definitions of the anatomic regions were based on those used for the Scheltens scale.²⁸ In short, the central sulcus acted as a dividing point between the frontal and parietal lobes down to the level at which the CC (splenium) became apparent. The Sylvian fissure functioned as the border between the frontal and the temporal lobe regions. The border between the basal ganglia and the temporal lobe was a straight line from the end of the Sylvian fissure to the cisterna ambiens. The infratentorial region was surrounded by CSF acting as the border. The division between the parietal and occipital region was defined on the basis of the parieto-occipital sulcus. For comparison, the group-averaged distribution of ARWMC is also illustrated in Fig 1.

Volumetric Assessment of Regional ARWMC Load. Volumetric analysis of ARWMC was performed on axial FLAIR images by using a semiautomated volume measurement based on local thresholding.²⁹ The analysis was performed by a single rater (E.C.W.v.S.) who was blinded to clinical details. This rater had previously evaluated other datasets and was experienced regarding both the software and the radiologic features. To achieve the volumetric assessment of regional ARWMC load, we normalized structural FLAIR and T2-weighted data to the standard T2-weighted template of SPM2 (<http://www.fil.ion.ucl.ac.uk/spm/spm2.html>) by using a 12-parameter affine transformation. A study-specific template was then created by averaging the normalized data and was used in a second pass to create the final

Table 2: Correlation coefficients (*r*) between CC areas and ARWMC volume measured in standard space*

Areas	Mean ARWMC (mL)	Mean CC Areas vs Mean ARWMC (mL) in the Brain (<i>r</i>)					
		CC1	CC2	CC3	CC4	CC5	CC Total
Mean CC area (mm ²)		179.3 ± 40.1	93.8 ± 25.2	90.8 ± 24.0	91.5 ± 27.3	184.0 ± 39.8	642.6 ± 135.4
ARWMC							
Basal ganglia region	0.7 ± 0.9	-0.111	-0.077	0.039	-0.038	-0.162‡	-0.095
Frontal lobes	14.7 ± 15.4	-0.181§	-0.078	0.027	-0.07	-0.232§	-0.144†
Occipital lobes	1.2 ± 1.6	-0.181‡	-0.107	-0.004	-0.04	-0.223§	-0.146†
Parietal lobes	6.0 ± 7.4	-0.137†	-0.097	-0.004	-0.067	-0.201§	-0.132†
Temporal lobes	1.3 ± 1.9	-0.154‡	-0.157‡	-0.067	-0.104	-0.206§	-0.168‡
Total ARWMC	24.0 ± 25.0	-0.175‡	-0.076	0.035	-0.042	-0.230§	-0.134†

Note:—CC indicates corpus callosum; ARWMC, age-related white matter changes.

* All CC and ARWMC values were normalized to the same head size. Values are mean CC areas and mean ARWMC volume (± SD), relative volume of the ARWMC volume assessed relative to the entire anatomic region, correlation coefficients (*r*), and significance level. In addition to the log-transformed ARWMC per brain region, we entered the following covariates: number of lacunes per brain region, number of infarcts, age, handedness, recruiting center, and ratings of sulcal and ventricular atrophy.

† *P* < .01.

‡ *P* < .001.

§ *P* < .0001 (uncorrected).

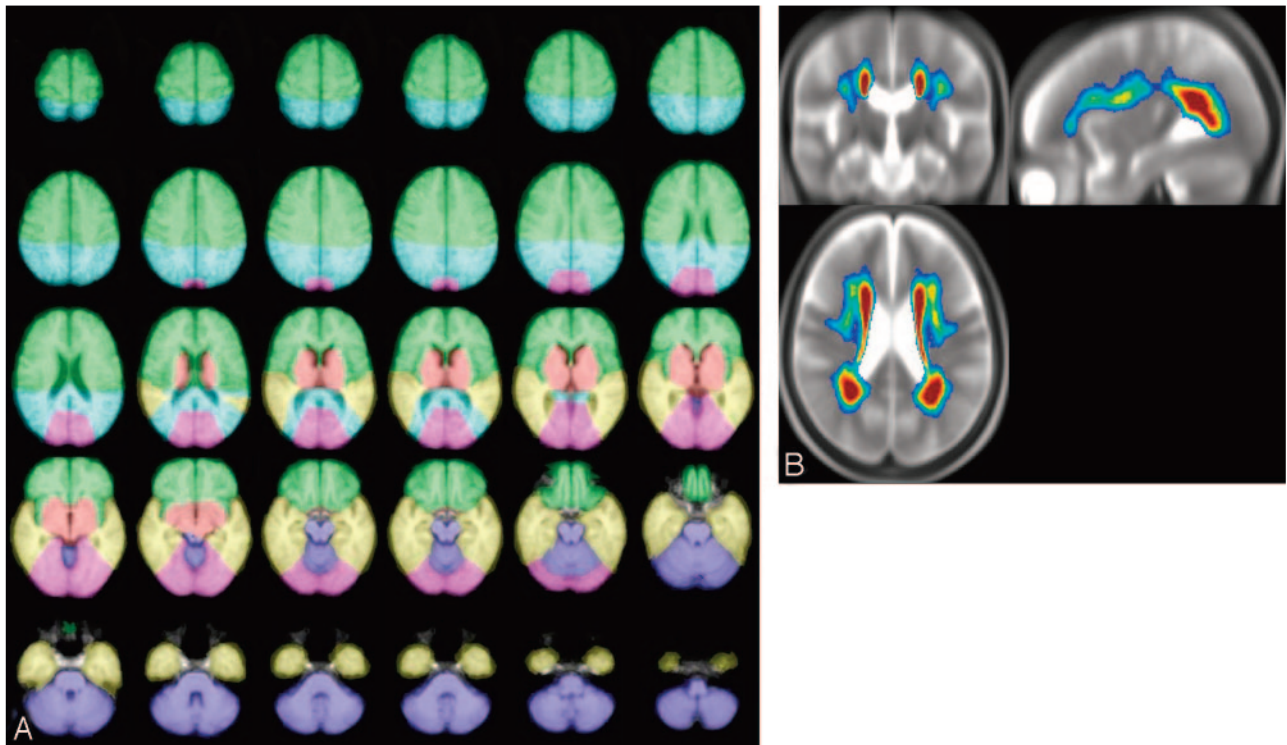


Fig 1. The left panel shows axial views illustrating the delineation of 6 anatomic regions: frontal (green), parietal (turquoise), temporal (yellow), basal ganglia (red), occipital lobes (pink), infratentorial regions (purple); see details in text. The right panel shows the average distribution of ARWMC projected onto orthogonal sections of the group-averaged T2-weighted image. The color-coding indicates the frequency of ARWMC occurrence, ranging from 5% (dark blue) to 30% and above (dark red).

normalized images. The delineated regions were transferred to the study-specific template by using 12-parameter spatial transformations. For each subject, the regional volume of ARWMC could then be calculated by combining the anatomic regions and the semiautomatically delineated ARWMC regions by using the logical “and” operation.

The Fazekas Rating Scale. Visual rating of the changes in cerebral subcortical white matter (from mild to severe) was determined on the FLAIR images by using a revised version of the Fazekas rating scale.²⁶ The scale includes score 1 (mild, single lesions <10 mm and areas of “grouped” ARWMC <20 mm in any diameter); score 2 (moderate, single hyperintensities between 10 and 20 mm; areas of grouped lesions >20 mm in diameter and no more than “connecting bridges” between individual lesions); and 3 (severe, single lesions or confluent areas of ARWMC ≥20 mm in

diameter). All ratings were performed by an experienced rater (E.C.W.v.S.) blinded to the clinical data.

Assessment of Lacunes and Infarcts. For the subsequent statistical analysis, the number of infarcts and lacunes was used as covariates. Lacunes were defined as hypointense foci ≥3 mm on MPRAGE that were surrounded by subcortical gray matter or white matter and not located in areas of a high frequency of widened perivascular spaces.³⁰ Infarcts were also counted (Table 1), and the assessment was performed by the same rater who evaluated ARWMC volumes and ratings.

Assessment of General Atrophy. To ascertain the independent effect of ARWMC on CC atrophy, we obtained measures of global atrophy. Ventricular and sulcal atrophy was rated separately by using a template-based rating scale ranging from 1 (no atrophy) to 8 (severe atrophy). This rating scale was developed and validated for FLAIR scans, because these are generally most likely to be present in all pa-

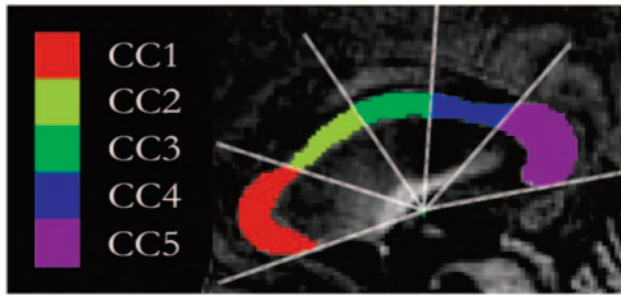


Fig 2. Segmentation and subdivision of the CC area into 5 distinct subregions obtained from the normalized midsagittal T1 (MPRAGE) scans. A radial partitioning scheme is used for regional analyses of the CC. CC1 indicates rostrum and genu; CC2, rostral body; CC3, midbody; CC4, isthmus; CC5, splenium.

tients, regardless of whether the study is a prospective trial or a retrospective survey. Intrarater repeatability was assessed on the basis of double readings of 50 randomly selected scans. Similarly, inter-rater repeatability was assessed from the readings of the same scans by 3 other persons.

For the current observer (R.S.), the intrarater κ value was >0.9 for both sulcal and ventricular atrophy; in general, the inter-rater κ value was 0.70 for sulcal and 0.83 for ventricular atrophy.

CC Area Measurement

The CC was automatically segmented and subsequently fully automatically divided into distinct subregions (Fig 2) according to a fixed scheme, as described in detail in a previous publication.⁴ Briefly, to measure the CC area, we stereotactically normalized all MPRAGE images to a reference T1-weighted image positioned in Talairach orientation³¹ with a 12-parameter affine transformation to correct for interindividual variability in the brain size and orientation. For each subject, the results of the normalization to parenchymal brain volume were checked manually by comparing the location of 6 marker points on the surface of the brain in relation to the template.

The CC was localized in an automatic way on the midsagittal section of the MPRAGE dataset by using the learning-based Active Appearance Models.³² An expert reviewer unaware of the clinical status subsequently corrected for any inaccuracies. Finally, the CC was automatically divided into 5 subregions. To find a suitable origin for the radial dividers, one rotates the CC into a coordinate system in which the x-axis is parallel to the longest axis (the first principal axis) of the structure and divides it into fractions containing the superior 95% and inferior 5% of the total area; the y-axis of the coordinate system passes through the center of gravity. Radial dividers with equal angular spacing were used to subdivide the CC into rostrum and genu (CC1), rostral body (CC2), midbody (CC3), isthmus (CC4), and splenium (CC5). The area of each segment was calculated automatically. Furthermore, to better illustrate the regional specificity between CC atrophy and ARWMC, we subdivided the CC into 10 regions by using a similar method (Fig 3).

Statistical Analysis

The correlation of the total and 5 regional CC areas with regionalized ARWMC load was examined by using the General Linear Model (GLM), adjusted for age, recruiting center, handedness, number of infarcts, and number of regional lacunes (Table 2). The visual scores for sulcal and ventricular atrophy were also included as covariates. Data from the infratentorial region were not analyzed because of the scarcity of ARWMC. Furthermore, due to the skewness of the distribution, the ARWMC load was calculated as the natural logarithm of the ARWMC volume. Hand-

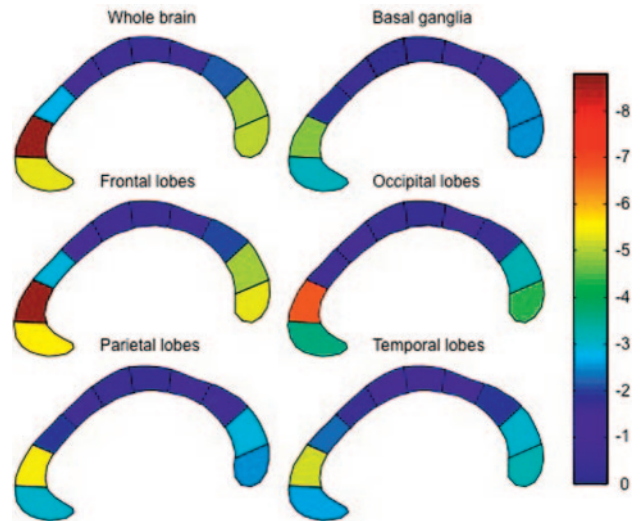


Fig 3. The correlation between the area of each of the 10 CC subregions and the volume of ARWMC in each of 5 hemispheric regions and the whole brain. To obtain a better illustration of the regional specificity between CC atrophy and ARWMC, we subdivided the CC into 10 subregions and not 5 subregions as reported in Fig 2. The color code from blue to red indicates the magnitude of regression coefficients.

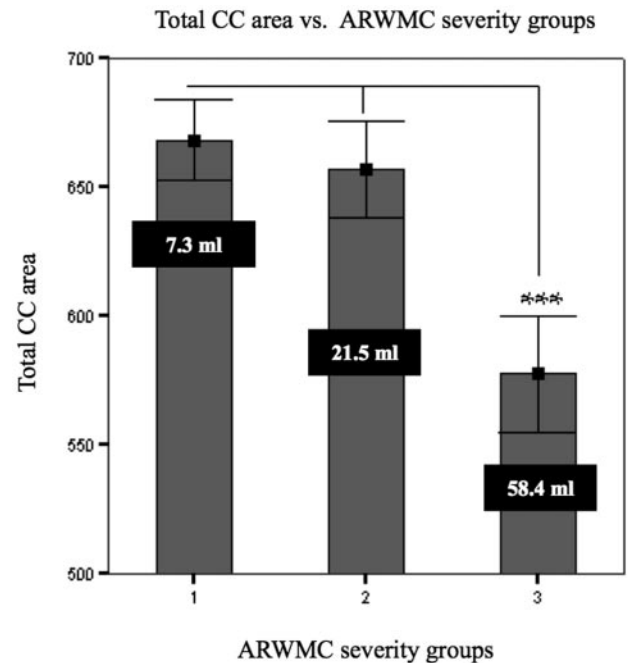


Fig 4. Comparison of mean total callosal area measured on normalized MR imaging in nondisabled elderly subjects, classified by severity of ARWMC (Fazekas ratings 1, 2, and 3). Vertical bars indicate SDs. The white figures indicate the mean ARWMC volumes. Triple asterisks indicate $P < .001$ (ANOVA test).

edness correction was performed because there is evidence that the CC is larger in left-handers, independent of cognitive function.¹⁵ Analysis of variance (ANOVA) was used to compare differences in mean total CC areas for subjects rated according to the Fazekas scale (Fig 4).

Furthermore, a color-coded diagram of the CC was made (Fig 3). The CC was color-coded from blue, to green, to yellow, to red with respect to the magnitude of the regression coefficients between the ARWMC load in the different brain regions and the areas of the CC subregions, resulting from the GLM described previously.

All statistical analyses were carried out by using the Statistical Package

for the Social Sciences software, Version 12 (SPSS, Chicago, Ill), and a value of $P < .05$ was considered statistically significant for individual comparisons. In the main analysis of CC subregions versus regional ARWMC load, a total of 36 regression analyses were performed, and a strict Bonferroni correction would, therefore, lead to a significance threshold of $P < .0014$. However, this is an estimate of the lower bound of the threshold because these comparisons are not independent.

Results

Patient Characteristics and ARWMC Ratings

Patient characteristics are summarized in Table 1. There were 578 subjects (313 women). Their mean age was 74 ± 5 years, and their Mini-Mental State Examination score was 27 ± 2 . Of the 578 subjects, 524 were right-handed, 27 were left-handed, 26 were ambidextrous, and 1 subject was not classified. For most subjects ($n = 260$), the ARWMC were rated as grade 1 according to the Fazekas scale, 178 were rated as grade 2, and 140, as grade 3.

The mean total CC area was $643 \pm 135 \text{ mm}^2$, and the total mean volume of ARWMC in the brain was $24.0 \pm 25.0 \text{ mL}$ (Table 2). Most ARWMC were found in the frontal lobe region ($14.7 \pm 15.4 \text{ mL}$).

Before we applied ANOVA and subsequently the GLM, the One-Sample Kolmogorov-Smirnov Test verified normal distribution of all CC areas and log-transformed ARWMC measurements in the basal ganglia, frontal lobes, occipital lobes, parietal lobes, and temporal lobes. An ANOVA test revealed that only subjects rated as grade 3 on the Fazekas scale had significantly smaller total CC areas ($P < .001$) relative to subjects rated as grades 1 and 2 (Fig 4).

In the GLM analysis, age, handedness, recruiting center, number of infarcts, number of lacunes, and ratings of sulcal and ventricular atrophy were entered as covariates. With the inclusion of these variables, there was a low but significant correlation between the total CC area and the total ARWMC load in the brain ($r = -0.13$; $P < .004$). More pronounced correlations were found for the rostral and splenium subregions (CC1 and CC5); most of these findings remained significant even with strict Bonferroni correction ($P < .0014$) (Table 2). For these subregions, the correlations were of similar magnitude for all regional ARWMC values; thus, they did not exhibit a regionally specific pattern. No significant correlations were found for the middle parts of CC (CC3 and CC4). All the significant results were in the expected direction (ie, high volume of ARWMC predicted small CC areas).

The overall pattern of the correlations is illustrated in Fig 3, showing the results of analyzing a finer subdivision of the CC with a similar GLM approach.

Among the other covariates entered, significant correlations were found only for the categorical variable "recruiting center" and for the rating of ventricular atrophy. Although the center effect was associated with all CC subregions, the effect of ventricular atrophy generally was only associated with CC1, CC4, CC5, and total CC-area. No significant correlations were found for age, handedness, number of infarcts, number of lacunes, or rating of sulcal atrophy.

Discussion

With data from 578 subjects, this is the largest study to date that investigated the association between ARWMC volume

and CC atrophy. We found that in nondisabled elderly subjects with very-mild-to-pronounced degrees of leukoaraiosis, there was a highly significant correlation between the total volume of ARWMC and rostral and splenium cross-sectional areas of the CC, indicating that increasing loads of ARWMC are associated with CC atrophy. This association remained significant after correction for a number of potential confounders, notably sulcal and ventricular atrophy.

For most brain regions (except the basal ganglia region), the volume of ARWMC was significantly correlated with the area of certain CC subregions, but we were unable to identify any regional specificity as regards the location of ARWMC. However, ARWMC seemed to be associated with CC tissue loss, mainly in the frontal and posterior part of the CC, whereas the size of the CC truncus was not associated with the volume of ARWMC.

Potential limitations of the present study should be mentioned. Most important, the regions chosen for ARWMC analysis may not well reflect the functional distribution of the CC axons. Furthermore, it is a cross-sectional study, and it is possible that a regional specificity of CC atrophy regarding the topographic location of ARWMC would have been better identified in a longitudinal design.

Nevertheless, our results are in accordance with the studies of Yamauchi et al (1994 and 1995).^{20,33} They reported that callosal atrophy occurs in patients with cerebrovascular disease. In contrast, Pantel et al (1998)³⁴ failed to demonstrate significant differences between vascular dementia and controls with respect to global and regional callosal size. This failure may be explained by a greater heterogeneity of the vascular dementia sample, which included patients with extensive white matter disease as well as patients with cortical infarcts.

In previous studies of patients with AD, a relationship between the ARWMC load and the size of the CC area was not clear.^{16,22} Meguro et al (2000)¹⁶ found that ARWMC were correlated with CC atrophy in healthy elderly subjects and in patients with AD. On the contrary, Teipel et al (1998)²² reported that ARWMC were not correlated with CC atrophy in patients with AD but only in healthy elderly adults.

The present study used a multicenter design that allowed the inclusion of a large cohort of patients at the price of some variability in the choice of scanning parameters. This variability may have led to center-specific effects that could influence the results to some extent. However, it should be noted that the main results were derived from semiautomated procedures that should be less susceptible to variability caused by minor differences in signal intensity. Furthermore, the recruiting center was included as a categorical variable in the statistical analysis, to minimize the risk of finding spurious associations caused by center-specific differences.

Earlier investigations of CC anatomy have been affected by methodologic weakness, including small sample sizes, different models for subdivision of CC, and analytic approaches that failed to account for the influences of other factors such as brain size and age. We used an automatic method for segmenting the CC, and this method, combined with a large sample size ($N = 578$) and statistical control for age, handedness, number of lacunes and infarcts, should give reliable results concerning ARWMC load and CC atrophy. All our CC measures were controlled for whole brain volume because the CC

assessment was normalized to parenchymal brain size. Therefore CC atrophy was not simply an element of diffuse brain atrophy. Furthermore, the use of quantitative measures may offer a better basis for investigation of the potential correlation between ARWMC in different brain regions and CC atrophy compared with different rating techniques.

The finding of a statistically significant impact of ARWMC load on CC atrophy was important and suggests that the volume of ARWMC is a predictor of CC atrophy. However, the correlation coefficients were small in absolute terms, showing that ARWMC is not the main determinant but that other factors, such as atrophy, may contribute to degeneration of the CC.

Furthermore, our study showed that in patients with severe ARWMC, a marked degeneration of the CC occurs. The coupling between ARWMC and CC atrophy suggests that subcortical changes have an effect on cortical connectivity in nondisabled elderly subjects with leukoaraiosis. Therefore, CC atrophy in this population may be an indicator for reduced neocortical functional integrity, which may be associated with some of the cognitive and motor deficits observed in this population.^{4,5}

Conclusion

In this large study of nondisabled elderly subjects with leukoaraiosis, increasing loads of ARWMC volume were significantly correlated with atrophy of the CC and its subregions. However, the correlation between ARWMC volume and CC subregions was not specifically related to the topographic location of ARWMC. The results suggest that ARWMC may be partly responsible for CC atrophy.

Future research could include other methods (ie, tractography) for investigating the potential topographic relationship between ARWMC and CC size. Furthermore, prospective longitudinal studies of increasing ARWMC load and regional atrophy on the CC structure and function should be performed.

Appendix: List of Participating Centers and Personnel

Helsinki, Finland (Memory Research Unit, Department of Clinical Neurosciences, Helsinki University): Timo Erkinjuntti, MD, PhD, Tarja Pohjasvaara, MD, PhD, Pia Pihanen, MD, Raija Ylikoski, PhD, Hanna Jokinen, PhD, Meija-Marjut Somerkoski, MPsych, Riitta Mäntylä, MD, PhD, Oili Salonen, MD, PhD; Graz, Austria (Departments of Neurology and Radiology, Division of Neuroradiology, Medical University Graz): Franz Fazekas, MD, Reinhold Schmidt, MD, Stefan Ropele, PhD, Brigitte Rous, MD, Katja Petrovic, MagPsychol, Ulrike Garmehi, Alexandra Seewann, MD; Lisbon, Portugal (Serviço de Neurologia, Centro de Estudos Egas Moniz, Hospital de Santa Maria): José M. Ferro, MD, PhD, Ana Verdelho, MD, Sofia Madureira, PsyD, Carla Moleiro, PhD; Amsterdam, the Netherlands (Department of Radiology and Neurology, VU Medical Center): Philip Scheltens, MD, PhD, Ilse van Straaten, MD, Frederik Barkhof, MD, PhD, Alida Gouw, MD, Wiesje van der Flier, PhD; Goteborg, Sweden (Institute of Clinical Neuroscience, Goteborg University): Anders Wallin, MD, PhD, Michael Jonsson, MD, Karin Lind, MD, Arto Nordlund, PsyD, Sindre Rolstad, PsyD, Ingela Isblad, RN; Huddinge, Sweden (Karolinska Institute, Neurotec Department, Sektion of Clinical Geriatrics): Lars-Olof Wahlund, MD, PhD,

Milita Crisby, MD, PhD, Anna Pettersson, RPT, PhD, Kaarina Amberla, PsyD; Paris, France (Department of Neurology, Hôpital Lariboisière): Hugues Chabriat, MD, PhD, Karen Hernandez, psychologist, Annie Kurtz, psychologist, Dominique Hervé, MD, Sarah Benisty, MD, Jean Pierre Guichard, MD; Mannheim, Germany (Department of Neurology, University of Heidelberg, Klinikum Mannheim): Michael Hennerici, MD, Christian Blahak, MD, Hansjorg Baezner, MD, Martin Wiarda, PsyD, Susanne Seip, RN; Copenhagen, Denmark (Memory Disorders Research Group, Department of Neurology, Rigshospitalet, and the Danish Research Center for Magnetic Resonance, Hvidovre Hospital, Copenhagen University Hospitals): Gunhild Waldemar, MD, DMSc, Egill Rostrup, MD, DMSc; Charlotte Ryberg, MSc, Tim Dyrby MSc, Olaf B. Paulson, MD, DMSc; Newcastle-upon-Tyne, UK (Institute for Ageing and Health, University of Newcastle): John O'Brien, DM, Sanjeet Pakrasi, MRCPsych, Mani Krishnan, MRCPsych, Andrew Teodorczuk, MRCPsych, Michael Firbank, PhD, Philip English, DCR, Thais Minett, MD, PhD. The Coordinating Center is in Florence, Italy (Department of Neurologic and Psychiatric Sciences, University of Florence): Domenico Inzitari, MD (Study Coordinator), Luciano Bartolini, PhD, Anna Maria Basile, MD, PhD, Eliana Magnani, MD, Monica Martini, MD, Mario Mascalchi, MD, PhD, Marco Moretti, MD, Leonardo Pantoni, MD, PhD, Anna Poggesi, MD, Giovanni Pracucci, MD, Emilia Salvadori, PhD, Michela Simoni, MD.

The LADIS Steering Committee includes Domenico Inzitari, MD (study coordinator); Timo Erkinjuntti, MD, PhD; Philip Scheltens, MD, PhD; Marieke Visser, MD, PhD; and Peter Langhorne, MD, BSc, PhD, FRCP, who replaced, in this role, Kjell Asplund, MD, PhD, beginning in 2005.

Acknowledgment

We thank Mikkel Stegmann, MSc, PhD, for development of software used for segmentation of the CC.

References

1. Hampel H, Teipel SJ, Alexander GE, et al. **Corpus callosum atrophy is a possible indicator of region- and cell type-specific neuronal degeneration in Alzheimer disease: a magnetic resonance imaging analysis.** *Arch Neurol* 1998;55:193–98
2. Moretti M, Carlucci G, Di CA, et al. **Corpus callosum atrophy is associated with gait disorders in patients with leukoaraiosis.** *Neurol Sci* 2005;26:61–66
3. Lyoo IK, Satlin A, Lee CK, et al. **Regional atrophy of the corpus callosum in subjects with Alzheimer's disease and multi-infarct dementia.** *Psychiatry Res* 1997;74:63–72
4. Ryberg C, Rostrup E, Stegmann MB, et al. **Clinical significance of corpus callosum atrophy in a mixed elderly population.** *Neurobiol Aging* 2007;28:955–63
5. Jokinen H, Ryberg C, Kalska H, et al. **Corpus callosum atrophy is associated with mental slowing and executive deficits in subjects with age-related white matter hyperintensities: the LADIS Study.** *J Neurol Neurosurg Psychiatry* 2007;78:491–96. Epub 2006 Oct 6
6. Pujol J, Vendrell P, Junque C, et al. **When does human brain development end? Evidence of corpus callosum growth up to adulthood.** *Ann Neurol* 1993;34:71–75
7. Kertesz A, Polk M, Carr T. **Cognition and white matter changes on magnetic resonance imaging in dementia.** *Arch Neurol* 1990;47:387–91
8. Highley JR, Esiri MM, McDonald B, et al. **The size and fibre composition of the corpus callosum with respect to gender and schizophrenia: a post-mortem study.** *Brain* 1999;122(pt 1):99–110
9. Byne W, Bleier R, Houston L. **Variations in human corpus callosum do not predict gender: a study using magnetic resonance imaging.** *Behav Neurosci* 1988;102:222–27
10. Salat D, Ward A, Kaye JA, et al. **Sex differences in the corpus callosum with aging.** *Neurobiol Aging* 1997;18:191–97

11. Steinmetz H, Jancke L, Kleinschmidt A, et al. **Sex but no hand difference in the isthmus of the corpus callosum.** *Neurology* 1992;42:749–52
12. O’Kusky J, Strauss E, Kosaka B, et al. **The corpus callosum is larger with right-hemisphere cerebral speech dominance.** *Ann Neurol* 1988;24:379–83
13. Kertesz A, Polk M, Howell J, et al. **Cerebral dominance, sex, and callosal size in MRI.** *Neurology* 1987;37:1385–88
14. Nasrallah HA, Andreasen NC, Coffman JA, et al. **A controlled magnetic resonance imaging study of corpus callosum thickness in schizophrenia.** *Biol Psychiatry* 1986;21:274–82
15. Witelson SF. **The brain connection: the corpus callosum is larger in left-handers.** *Science* 1985;229:665–68
16. Meguro K, Constans JM, Courtheoux P, et al. **Atrophy of the corpus callosum correlates with white matter lesions in patients with cerebral ischaemia.** *Neuroradiology* 2000;42:413–19
17. van Swieten JC, van den Hout JH, van Ketel BA, et al. **Periventricular lesions in the white matter on magnetic resonance imaging in the elderly: a morphometric correlation with arteriolosclerosis and dilated perivascular spaces.** *Brain* 1991;114(pt 2):761–74
18. Witelson SF. **Hand and sex differences in the isthmus and genu of the human corpus callosum: a postmortem morphological study.** *Brain* 1989;112(pt 3):799–835
19. Quint DJ. **Multiple sclerosis and imaging of the corpus callosum.** *Radiology* 1991;180:15–17
20. Yamauchi H, Fukuyama H, Ogawa M, et al. **Callosal atrophy in patients with lacunar infarction and extensive leukoaraiosis: an indicator of cognitive impairment.** *Stroke* 1994;25:1788–93
21. Vermersch P, Roche J, Hamon M, et al. **White matter magnetic resonance imaging hyperintensity in Alzheimer’s disease: correlations with corpus callosum atrophy.** *J Neurol* 1996;243:231–34
22. Teipel SJ, Hampel H, Alexander GE, et al. **Dissociation between corpus callosum atrophy and white matter pathology in Alzheimer’s disease.** *Neurology* 1998;51:1381–85
23. Teipel SJ, Bayer W, Alexander GE, et al. **Progression of corpus callosum atrophy in Alzheimer disease.** *Arch Neurol* 2002;59:243–48
24. Yamauchi H, Fukuyama H, Shio H. **Corpus callosum atrophy in patients with leukoaraiosis may indicate global cognitive impairment.** *Stroke* 2000;31:1515–20
25. Pantoni L, Basile AM, Pracucci G, et al. **Impact of age-related cerebral white matter changes on the transition to disability: the LADIS study—rationale, design and methodology.** *Neuroepidemiology* 2005;24:51–62
26. Lawton MP, Brody EM. **Assessment of older people: self-maintaining and instrumental activities of daily living.** *Gerontologist* 1969;9:179–86
27. Fazekas F, Chawluk JB, Alavi A, et al. **MR signal abnormalities at 1.5 T in Alzheimer’s dementia and normal aging.** *AJR Am J Roentgenol* 1987;149:351–56
28. Scheltens P, Barkhof F, Leys D, et al. **A semiquantitative rating scale for the assessment of signal hyperintensities on magnetic resonance imaging.** *J Neurol Sci* 1993;114:7–12
29. van Straaten EC, Fazekas F, Rostrup E, et al. **Impact of white matter hyperintensities scoring method on correlations with clinical data: the LADIS study.** *Stroke* 2006;37:836–40. Epub 2006 Jan 26
30. van Straaten EC, Scheltens P, Knol DL, et al. **Operational definitions for the NINDS-AIREN criteria for vascular dementia: an interobserver study.** *Stroke* 2003;34:1907–12. Epub 2003 Jul 10
31. Talairach J, Tournoux P. *Co-Planar Stereotaxic Atlas of the Human Brain.* New York: Thieme, 1988
32. Cootes TF, Edwards GJ, Taylor CJ. **Active appearance models.** *IEEE Trans Pattern Anal Mach Intell* 2001;23:681–85
33. Yamauchi H, Pagani M, Fukuyama H, et al. **Progression of atrophy of the corpus callosum with deterioration of cerebral cortical oxygen metabolism after carotid artery occlusion: a follow up study with MRI and PET.** *J Neurol Neurosurg Psychiatry* 1995;59:420–26
34. Pantel J, Schroder J, Essig M, et al. **Corpus callosum in Alzheimer’s disease and vascular dementia: a quantitative magnetic resonance study.** *J Neural Transm Suppl* 1998;54:129–36